# Relation between crystal symmetry and ionicity in silica polymorphs

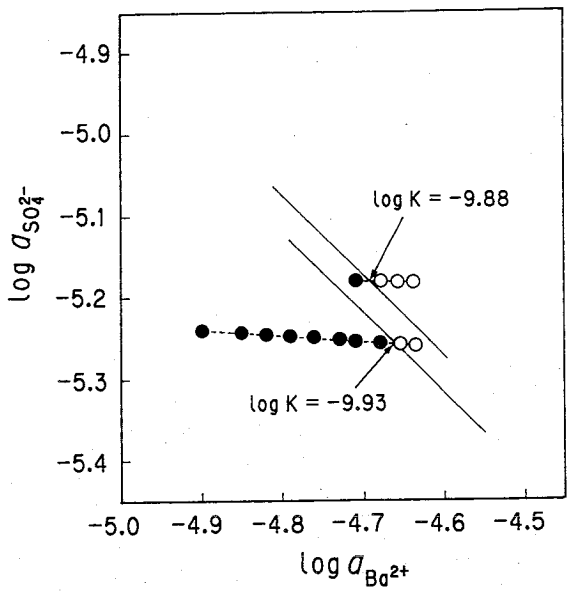


FIG. 4 Relationships between surface dissolution phenomena of a barite crystal and the composition (the activities of $Ba^{2+}$ and $SO_4^{2-}$) of experimental solutions containing 3M NaCl at $T = 150 \pm 0.5$ °C. The solution composition was changed successively by addition of $BaCl_2$ titrant. The activity values for $Ba^{2+}$ and $SO_4^{2-}$ were computed from the molalities of ΣBa, $\Sigma SO_4^{2-}$, ΣNa, and ΣCl of the experimental solutions using the extended Debye–Hückel method. The solid symbols represent the conditions where dissolution phenomena were recognized; the open symbols where no dissolution phenomenon was observed in 6 hours. Solid lines represent two values of log $K$ where $K = a_{Ba^{2+}} a_{SO_4^{2-}}$.

observed in 12 hours at the 'end points' of the titration, the Ω values of the 'end-point' solutions must be greater than 0.999, and possibly greater than 1.0 (supersaturation). Reversal of the dissolution process (in other words, crystal growth) using the same crystal was not detected until the Ω value exceeded 1.26 (see point Cg in Fig. 2), probably because many of the crystal defects, which could become nucleation sites, had been dissolved away during the earlier reactions with undersaturated solutions. When the 'old' gypsum crystal was replaced by a 'fresh' one at the saturation point and the titration was continued, some crystal growth features were recognized at $\Omega \geq 1.06$ (see point Cn in Fig. 2). These experiments indicate that the end points (equilibrium values) of solution–solid reactions can be determined much more precisely by observing dissolution rather than growth phenomena of crystals.

Figure 4 is an example of results from our experiments on dissolution of barite in a 3M NaCl solution at 150 °C using the experimental system shown in Fig. 1. The equilibrium constant for dissociation of barite, $\log K = \log a_{Ba^{2+}} + \log a_{SO_4^{2-}}$, is found to be $-9.90 \pm 0.03$ at 150 °C from our two series of experiments (K.H. *et al.*, manuscript in preparation). In comparison, the log $K$ value at 150 °C based on the experimental data of Blount[6] on the solubility of barite in NaCl solutions and on more recent thermodynamic data (see ref. 7 for summary) for the aqueous species ranges from −9.5 to −10.2. Blount[6] required run times of several weeks to demonstrate equilibrium between barite and aqueous solution at temperatures around 150 °C, and the experimental solutions had to be analysed for barium and/or sulphate. In contrast, our two series of barite experiments (Fig. 4) were completed in less than 2 days, and a chemical analysis of the experimental solution was not necessary, demonstrating some of the advantages of our experimental method.

Barite is one of the least soluble minerals in nature; its solubility is about three orders of magnitude lower than that of gypsum at room temperature[4,5]. The two examples given (gypsum at 25 °C and barite at 150 °C) illustrate that the method described here is applicable to studies aimed at obtaining precise data on the solubility and reaction kinetics of a wide variety of solution-solid reactions, including those with very low solubility, over wide ranges of temperature and pressure. □

Received 23 January; accepted 29 April 1991.

1. Ulmer, G. C. & Barnes, H. L. (eds) *Hydrothermal Experimental Techniques* (Wiley, New York, 1987).
2. Tsukamoto, K. *J. Cryst. Growth* **61**, 199–209 (1983).
3. Tsukamoto, K. & Sunagawa, I. *J. Cryst. Growth* **71**, 183–190 (1985).
4. Blount, C. W. & Dickson, F. W. *Am. Miner.* **58**, 323–331 (1973).
5. Holland, H. D. & Malinin, S. D. in *Geochemistry of Hydrothermal Ore Deposits* 2nd ed (ed. Barnes, H. L.) 461–508 (Wiley, New York, 1979).
6. Blount, C. W. *Am. Miner.* **62**, 942–957 (1977).
7. Ohmoto, H. *et al. Econ. Geol.* **5**, 570–604 (1983).

ACKNOWLEDGEMENTS. We thank M. Matsubara and S. Sugino for technical assistance in the development of the experimental system, and S. L. Brantley, A. C. Lasaga, M. J. Machesky, S. R. Poulson and D. K. Smith for useful comments on an earlier manuscript. This work was supported by the Japanese Ministry of Education, Science and Culture and the NSF.

# Relation between crystal symmetry and ionicity in silica polymorphs

**G. J. Kramer*, B. W. H. van Beest* & R. A. van Santen*†**

* Koninklijke/Shell-Laboratorium, Amsterdam (Shell Research B.V.), PO Box 3003, 1003 AA Amsterdam, The Netherlands
† Schuit Institute of Catalysis, Laboratory of Inorganic Chemistry and Catalysis, Eindhoven University of Technology, PO Box 513, 5600 MB Eindhoven, The Netherlands

**THE structure and stability of an inorganic solid is determined in general both by short-range covalent and by long-range electrostatic forces. Here we describe the use of interatomic force fields developed recently from first-principles quantum-chemical cluster calculations[1,2] in the study of the structures of $SiO_2$ tetrahedral networks. We find that the symmetry of these structures depends sensitively on the balance between ionic and covalent forces: high-symmetry structures are stabilized for relatively large ion partial charges, and low-symmetry structures are stabilized when the ionicity is small. For some $SiO_2$ polymorphs, the low-symmetry structures found in our simulations correspond to the low-temperature phases of these polymorphs found experimentally. A reinterpretation of structural data on quartz provides evidence for temperature dependence of the ionicity, which can explain the change of symmetry observed when temperature is increased. Our preliminary calculations on aluminophosphates suggest that this symmetry-breaking mechanism may also provide insight into the structural changes observed for complex molecular sieves.**

The theoretical study of silicas has advanced to the point where the properties of the simplest structures can be calculated from first principles using quantum chemical tools[3,4]. The study of silicas and silicates with large unit cells, such as zeolites, as well as the study of minerals, has relied on methods that describe the interaction between atoms in these (partially) ionic solids by empirical potentials or force fields; a review is given in ref. 5. Only recently, though, have force-field descriptions based on *ab initio* calculations been proposed for mixed ionic–covalent systems such as silicas[1,2,6,7] and aluminophosphates[1,2]. The advantage of the latter approach over the empirical approach lies in the first-principles description of the silicon–oxygen bond and of the repulsion between neighbouring oxygen atoms. A molecular dynamics study by Tsuneyuki *et al.* employing such a force field has reproduced the various $SiO_2$ polymorphs as thermodynamically stable systems[7,8].

In spite of their foundation in *ab initio* quantum chemistry, force-field methods are ultimately empirical: there is no *a prior*

preferred functional form, and the treatment of the atoms as point-like, charged particles is an abstraction, as a consequence of which the magnitude of the charge is not uniquely defined. This fact, in combination with the infinite range of the electrostatic interactions, precludes the derivation of accurate force fields solely from the potential-energy surface of clusters[1,2]. But the success of force fields based on *ab initio* calculations on small clusters ($SiO_4$ or $Si(OH)_4$, refs 7 and 1 respectively) in the prediction of properties directly related to the Si–O bonding, such as the vibrational frequencies of quartz[2], does indicate that the covalent bonding is correctly described by such methods. Here we will exploit this fact and, at the same time, use the indeterminacy of Coulomb interactions to study the effect of changes in the balance between covalent and ionic interactions on the structure of $SiO_2$ polymorphs, in particular with respect to crystal symmetry.

We have performed a series of lattice-energy-minimization calculations on each of five $SiO_2$ polymorphs (quartz, cristobalite, coesite, stishovite and silicalite) using force fields, based on first principles, which differ in ionicity. The effective charge on silicon ($Q_{Si}$) is varied between 2 and 3 (at 0.1 or 0.2 intervals), and is thus significantly smaller than the formal silicon charge of 4, thereby complying with the mixed ionic–covalent character of the system. For each choice of $Q_{Si}$, parameters of the short-range force field have been determined that fit the potential energy surface of the $Si(OH)_4$ molecule. This ensures the correct description of the covalent interactions within the $SiO_4$ tetrahedron for all choices of $Q_{Si}$.

The crystal symmetry of the systems as modelled can be read from the calculated unit-cell matrix and from the elasticity matrix[9] or the bulk modulus. Figure 1 shows the dependence of the calculated bulk modulus on $Q_{Si}$. Between $Q_{Si}=2.4$ and $Q_{Si}=2.6$, the bulk moduli of quartz, cristobalite and silicalite (the all-silica form of zeolite ZSM-5) (ref. 10) show a sudden change, which reflects a change of symmetry. For quartz, the low-$Q_{Si}$ phase corresponds to low quartz or $\alpha$-quartz; the high-$Q_{Si}$ phase is high quartz or $\beta$-quartz. For cristobalite the same symmetry breaking occurs, and for silicalite the high-$Q_{Si}$ structure is orthorhombic and the low-$Q_{Si}$ structure triclinic. The symmetries of the energy-minimized structures of coesite and stishovite are not affected.

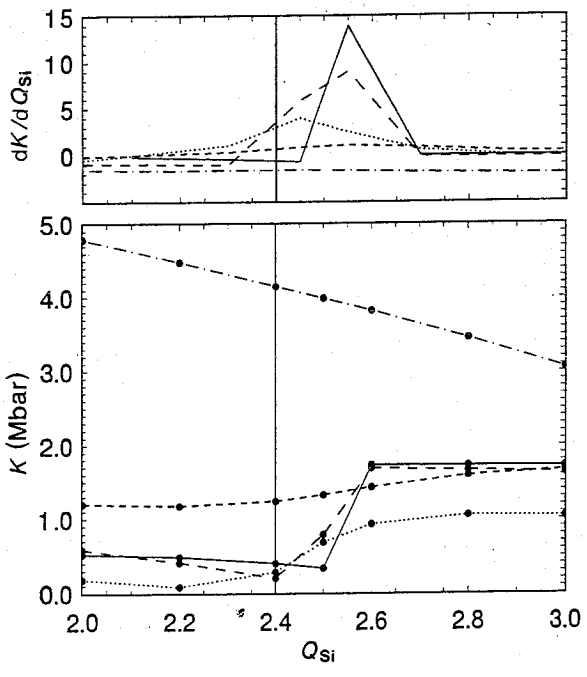


FIG. 1 Calculated bulk moduli ($K$) plotted against silicon charge for quartz (——), cristobalite (– – –), coesite (- - - -), silicalite (·····) and stishovite (—·—). The force field with $Q_{Si}=2.4$ gives the best description of the low-temperature structure and elastic properties of $\alpha$-quartz. The transitions from low to high symmetry occur roughly at $Q_{Si}=2.5$, as can be seen clearly from the numerical derivatives ($dK/dQ_{Si}$).

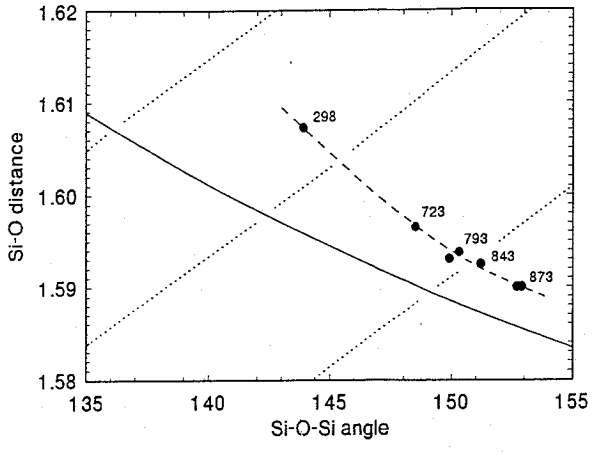


FIG. 2 Experimental relation between Si–O distance and Si–O–Si angle for quartz at different temperatures (circles; the dashed line is a guide to the eye), compared with the theoretical prediction as obtained from STO3G calculations on the disilanol molecule (solid line). The dotted curves are lines of equal Mulliken charge (top left, 1.35, to bottom right, 1.37).

These computer simulations bear an intriguing resemblance to the actual crystal symmetry found in nature. The low-$Q_{Si}$ phases correspond to the low-temperature phases of silica ($\alpha$-quartz, low cristobalite and monoclinic silicalite), and the high-$Q_{Si}$ values correspond to the high-temperature phases $\beta$-quartz ($T>853$ K; ref. 11), high-cristobalite ($T>493$ K; ref. 12) and orthorhombic silicalite ($T>628$ K; ref. 13). Coesite and stishovite, for which no structural phase transitions are known, do not display any ionicity-induced changes in our simulations.

This striking similarity suggests a coupling between the ionicity of silicas and temperature. Evidence for such a coupling can be found from a combination of experimental information on quartz and *ab initio* calculations on small clusters.

The crystallographic study of quartz at elevated temperatures[14] has revealed that, as the temperature is raised from 293 to 873 K, the Si–O–Si angle ($\theta$) increases steadily from 144 to 153°. Such an increase is to be expected because the low-energy phonons of quartz (or any other silica) have primarily a bond-bending character[15]. Coupled to the increase in bonding angle, the bond distance decreases from 1.607 to 1.590 Å (see Fig. 2). This negative coupling is the result of the changing hybridization on the oxygen atoms. *Ab initio* calculations on disilanol ($H_6Si_2O_7$)[16] reveal a low-energy valley running diagonally across the (bond-angle, bond-length) (Fig. 2). Along this valley, the ionicity of the disilane molecule increases with the bonding angle. This is seen from changes in the charge on silicon, as calculated from the occupation of the silicon atomic orbitals (Mulliken charge), which increases by ~0.02$e$, where $e$ is the charge on an electron, on silicon. This effect will be amplified in bulk silica, where all Si–O–Si angles around silicon are increased, instead of just one, as in the disilanol cluster. Therefore, in bulk silica the change in effective charge on silicon may be as large as 0.1$e$. This value is roughly equal to the difference (in $Q_{Si}$) between the ionicity of the low-temperature force field ($Q_{Si}=2.4$) and the phase boundary between low- and high-symmetry structures ($Q_{Si}\approx 2.55$). It is important that both ionicity differences are of the same order of magnitude. Numerical correspondence is not expected, as the definitions of charge in the molecular calculations and in the force-field calculations differ, demonstrating the ambiguity in the definition of point charges mentioned earlier.

As force-field modelling of quartz[1,2] has shown that the balance between ionic and covalent forces of the force field that

best describes $\alpha$-quartz is very close to a transition to $\beta$-quartz, we conclude that the high-temperature, $\beta$ phase of quartz is an 'ionicity-stabilized' phase. This conclusion contrasts with the findings of a molecular-dynamics study by Tsuneyuki *et al.*[17], who conclude that $\beta$-quartz is a dynamic phase, oscillating in between the two chirally opposite realizations of $\alpha$-quartz symmetry. In the latter picture it is difficult to explain the existence of an intermediate, incommensurate phase of quartz in an interval of 1.8 K near the transition temperature[18]. A Landau-type theory[19] gives a proper description of the $\beta$-to-incommensurate transition, explicitly requiring a $\beta$ phase characterized by a single minimum.

The striking similarity between the transitions in quartz, cristobalite and zeolite MFI, both in simulation and in the observed character of the transition, leads us to conclude that the phase transitions have the same origin: an increased ionicity of the system induced by the increased angle of bonding on oxygen.

Here we are dealing with subtle changes in the crystal symmetry, but it is worth noting that a correspondence between ionicity and atomic coordination has been found previously. As pointed out by Phillips[20], binary semiconductors show a change from fourfold to sixfold coordination with increasing ionicity.

We have carried our simulation one step further, to the study of aluminophosphates (ALPOs). In our simulations we can reproduce the $\alpha$-to-$\beta$ transition in berlinite (ALPO quartz) which is analogous to that in quartz, by increasing the relative strength of electrostatic interactions in the ALPO system. Moreover, analogous transitions occur, for example, in the open molecular-sieve-type networks of VPI-5 (ref. 24) and ALPO-8. Here, the symmetry breaking has a remarkable geometric consequence: the layers that form the structure shift perpendicular to the crystallographic $c$ axis, thereby rendering the channels slightly sinusoidal. In both cases, recent structural studies[21–23] have indeed revealed such deformations, which are not present in the idealized network geometries suggested originally[24].

*Note added in proof.* A recent paper[25] provides experimental evidence that the $\alpha$-$\beta$ phase transition in quartz is indeed a structural phase transition, as suggested here, rather than an order–disorder transition as suggested in ref. 17. □

Received 29 January; accepted 29 April 1991.


1. Van Beest, B. W. H., Kramer, G. J. & Van Santen, R. A. *Phys. Rev. Lett.* **64,** 1955–1958 (1990).
2. Kramer, G. J., Farragher, N. P., Van Beest, B. W. H. & Van Santen, R. A. *Phys. Rev.* B**43,** 5068–5080 (1991).
3. Dovesi, R., Pisani, C., Roetti, C. & Silvi, B. *J. chem. Phys.* **86,** 6967–6971 (1987).
4. Allan, D. C. & Teter, M. P. *Phys. Rev. Lett.* **59,** 1136–1139 (1987).
5. Catlow, R. C. A. & Price, G. D. *Nature* **347,** 243–248 (1990).
6. Lasaga, A. C. & Gibbs, G. V. *Phys. Chem. Miner.* **14,** 107–117 (1987).
7. Tsuneyuki, S., Tsukada, M., Aoki, H. & Matsui, Y. *Phys. Rev. Lett.* **61,** 869–872 (1988).
8. Tsuneyuki, S., Matsui, Y., Aoki, H. & Tsukada, M. *Nature* **339,** 209–211 (1989).
9. Nye, J. F. *Physical Properties of Crystals* (Oxford University Press, Oxford, 1957).
10. Meier, W. M. & Olson, D. H. *Atlas of Zeolite Structure Types,* 2nd edn (Butterworth, Cambridge, 1987).
11. Axe, J. D. & Shirane, G. *Phys. Rev.* B**1,** 342–348 (1970).
12. Peacor, D. R. *Z. Kristallogr.* **138,** 274–298 (1973).
13. Fyfe, C. A., Strobl, H., Kokotailo, G. T., Kennedy, G. J. & Barlow, G. E. *J. Am. chem. Soc.* **110,** 3373–3380 (1988).
14. Grimm, H. & Dorner, B. *J. Phys. Chem. Solids* **36,** 407–413 (1975).
15. Van Santen, R. A. & Vogel, D. L. *Adv. Solid St. Chem.* **1,** 151–224 (1989).
16. Lasaga, A. C. & Gibbs, G. V. *Phys. Chem. Miner.* **16,** 29–41 (1988).
17. Tsuneyuki, S., Aoki, H., Tsukada, M. & Matsui, Y. *Phys. Rev. Lett.* **64,** 776–779 (1990).
18. Gouhara, K. & Kato, N. *J. phys. Soc. Japan* **54,** 1868–1881; 1882–1889 (1985).
19. Mukamel, D. & Walker, M. B. *Phys. Rev. Lett.* **58,** 2559–2562 (1987).
20. Phillips, J. C. *Bonds and Bands in Semiconductors* (Academic, New York, 1973).
21. Dessau, R. M., Schlenker, J. L. & Higgins, J. B. *Zeolites* **10,** 522–524 (1990).
22. Rudolf, P. R. & Crowder, C. E. *Zeolites* **10,** 163–168 (1990).
23. McCusker, L. B., Baerlocher, C., Jahn, E. & Bülow, M. *Zeolites* (in the press).
24. Davis, M. E., Saldarriaga, C., Montes, C., Garces, J. & Crowder, C. *Zeolites* **8,** 362–366 (1988).
25. Tezuka, Y., Shin, S. & Ishigame, M. *Phys. Rev. Lett.* **66,** 2356 (1991).


# NMR evidence for five-coordinated silicon in a silicate glass at atmospheric pressure

**Jonathan F. Stebbins**

Department of Geology, Stanford University, Stanford, California 94305, USA

**KNOWLEDGE of the structure of liquid silicates is essential to understanding the properties of materials ranging from magmas in lava flows to melts in glass processing. At 1 atmosphere pressure, a wide range of evidence indicates that most silicon cations in these systems are coordinated by four oxygens in a tetrahedral configuration ($Si^{IV}$). Molecular dynamics computer simulations of these liquids have, however, predicted that defect complexes (of relatively low abundance) consisting of silicon with five oxygen neighbours ($Si^{V}$) are of key importance in the mechanism by which viscous flow takes place[1–5]. I present here direct experimental evidence from $^{29}Si$ NMR studies of $K_2Si_4O_9$ glass that $Si^{V}$ does exist in silicate liquids at low pressures, and that the abundance of this species increases with temperature, supporting the idea that $Si^{V}$ defects contribute to 'weakening' of the structure of molten silicates.**

Pressure-induced changes from $Si^{IV}$ to six-coordinated silicon ($Si^{VI}$) are well known in crystalline silicates, and most of the silicon in the deep interior of the earth is probably present in the latter state. Data from $^{29}Si$ magic angle spinning (MAS) NMR confirmed the beginning of this transformation in glasses quenched from alkali silicate liquids at pressures up to 12 GPa[6–8]. NMR peaks for $Si^{VI}$ with chemical shifts near to −200 p.p.m. were clearly observed, as seen previously in crystalline silicates

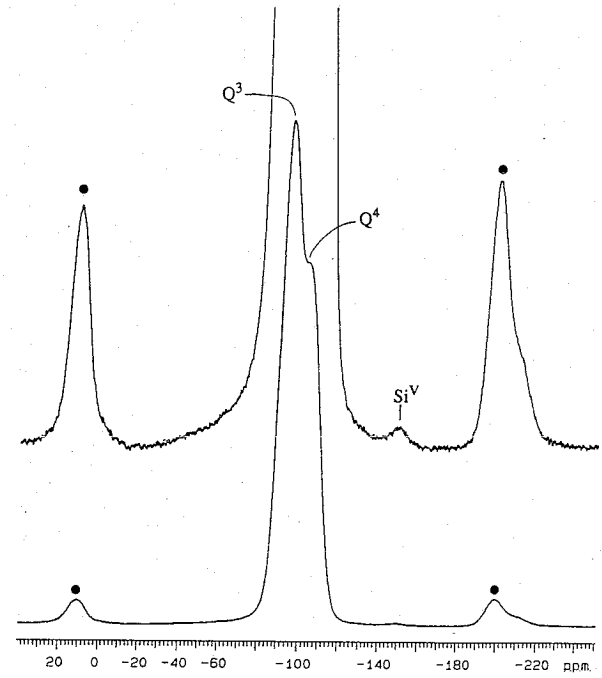


FIG. 1 The $^{29}Si$ MAS NMR spectrum for fast-quenched $K_2Si_4O_9$ glass. Upper trace is lower trace×10. Data were collected with a Varian VXR 400 spectrometer at a Larmor frequency of 79.5 MHz, using a high-speed MAS probe (Doty Scientific, Inc.) with a 5-mm rotor. A spin tip angle of 30° and a 1-s delay between pulses were used (using 10-s and 60-s delays produced no significant differences from the 1-s delay in the relative abundance of $Si^{V}$ sites). Data from ~50,000 pulses were averaged. A 20-Hz exponential line broadening was used to improve the signal-to-noise ratio. Frequency reference was tetramethyl silane. Solid circles mark spinning side bands.